ARTICLE
Journal of Cellular Biochemistry 115:585–595 (2014)

Journal of Cellular Biochemistry

Osteopontin Has a Crucial Role in Osteoclast-Like Multinucleated Giant Cell Formation

Yukiko Oh,[1]* Iekuni Oh,[2] Junko Morimoto,[3] Toshimitsu Uede,[3] and Akira Morimoto[1]

[1]*Department of Pediatrics, Jichi Medical University School of Medicine, 3311-1, Yakushi-ji, Shimotsuke, Tochigi 329-0498, Japan*

[2]*Department of Hematology, Jichi Medical University School of Medicine, 3311-1, Yakushi-ji, Shimotsuke, Tochigi 329-0498, Japan*

[3]*Division of Molecular Immunology, Institute for Genetic Medicine, Hokkaido University, Kita-15, Nishi-7, Kita-ku, Sapporo 060-0815, Japan*

ABSTRACT

The osteoclast (OC) is a major player in the pathogenic bone destruction of inflammatory bone diseases such as rheumatoid arthritis and Langerhans cell histiocytosis. Recently, it was shown that immature dendritic cells (iDC) fuse faster and more efficiently than monocytes in forming OC-like multinucleated giant cells (MGCs), and that osteopontin (OPN) is involved in the pathogenesis of inflammatory bone diseases. In this study, we hypothesized that OPN is a key factor for generation of OC-like MGCs from iDCs. We used an in vitro culture system to differentiate iDCs, derived from monocytes obtained from the blood of healthy donors, into OC-like MGCs. We evaluated OPN levels and expression of OPN receptors during the course of differentiation. OPN has an arginine-glycine-aspartic acid (RGD) motif, and protease cleavage reveals a SVVYGLR motif. The concentrations of both full-length and cleaved forms of OPN increased during the course of OC-like MGC formation. Expression of OPN RGD- and SVVYGLR-recognizing receptors also increased at later stages. We analyzed whether blocking OPN binding to its receptors affected OC-like MGC formation. Monocytes treated with OPN siRNA were able to differentiate into iDCs effectively; however, differentiation of these iDCs into OC-like MGCs was significantly reduced. The formation of OC-like MGCs was not significantly reduced by RGD synthetic peptide. By contrast, SVVYGLR synthetic peptide caused a significant reduction. These data suggest that the cleaved form of OPN plays a critical role in driving iDC differentiation into OC-like MGCs in the early phase of differentiation, in an autocrine and/or paracrine fashion. J. Cell. Biochem. 115: 585–595, 2014. © 2013 Wiley Periodicals, Inc.

KEY WORDS: OSTEOPONTIN; OSTEOCLAST; IMMATURE DENDRITIC CELL; MULTINUCLEATED GIANT CELL; INFLAMMATORY BONE DISEASE

Osteoclasts (OC) are bone-resorbing giant polykaryon cells that differentiate from mononuclear macrophage/monocyte-lineage hematopoietic precursors. Upon stimulation by cytokines, such as macrophage colony-stimulating factor (M-CSF) and receptor activator of NF-κB ligand (RANKL), OC precursor cells migrate and attach onto the bone surface. There they fuse with each other to form multinucleated giant cells (MGCs) and mediate bone resorption [Teitelbaum, 2000].

Osteopontin (OPN) plays an important role physiologically in bone remodeling, especially in bone resorption, by modulating OC function [Chellaiah et al., 2003; Standal et al., 2004]. OPN contains the classical cell-binding motif arginine-glycine-aspartic acid (RGD) that binds cell surface RGD-recognizing integrins such as αvβ1, αvβ3, α5β1, and CD44 variant (v) 6 [Hu et al., 1995; Gao et al., 2003]. RGD-recognizing integrins are expressed by a variety of cells including fibroblasts, smooth muscle cells, endothelial cells, epithelial cells, and immune cells [Uede, 2011]. OPN can be cleaved by proteases, including thrombin and plasmin, which exposes a serine-valine-valine-tyrosine-glycine-leucine-arginine (SVVYGLR) motif [Yokosaki et al., 1999]. This motif is recognized by non-RGD-recognizing integrins such as α4β1 expressed by T cells and macrophages, and α9β1 expressed by fibroblasts, neutrophils, macrophages, smooth muscle cells, and OCs [Smith et al., 1996; Green et al., 2001].

Grant sponsor: The Ministry of Health, Labor and Welfare, Japan; Grant sponsor: Japan Society for Promotion of Science (JSPS); Grant sponsor: Jichi Medical University Graduate Student Start-Up Grant for Young Investigators; Grant number: 22591167; Grant sponsor: Grant-in-Aid for Scientific Research (KAKENHI) from the Ministry of Education, Culture, Sports, Science and Technology, Japan; Grant sponsor: JKA Foundation.

*Correspondence to: Yukiko Oh, MD, Department of Pediatrics, Jichi Medical University School of Medicine, 3311-1, Yakushi-ji, Shimotsuke, Tochigi 329-0498, Japan. E-mail: yukikok@jichi.ac.jp

Manuscript Received: 16 May 2013; Manuscript Accepted: 10 October 2013

Accepted manuscript online in Wiley Online Library (wileyonlinelibrary.com): 15 October 2013

DOI 10.1002/jcb.24695 • © 2013 Wiley Periodicals, Inc.

OCs play a major role in the pathogenic bone destruction of rheumatoid arthritis (RA) and Langerhans cell histiocytosis (LCH) [Redlich et al., 2002; da Costa et al., 2005]. Recently, it was revealed that immature dendritic cells (iDC) fuse more quickly and efficiently than monocytes to form OC-like MGCs in the inflammatory environment [Rivollier et al., 2004]. This suggests that iDC-derived OCs may be directly involved in the osteolytic lesions observed in inflammatory bone diseases such as RA or LCH. OPN is implicated in the pathogenesis of RA [Yumoto et al., 2002; Yamamoto et al., 2007] and LCH [Prasse et al., 2009; Allen et al., 2010].

Based on these findings, we hypothesized that OPN is a key factor in the formation of OC-like MGCs from iDCs. In this study we found that OPN, particularly after cleavage, plays a critical role in the formation of OC-like MGCs from iDCs in an autocrine and paracrine manner.

MATERIALS AND METHODS

MONOCYTE PURIFICATION AND IDC DIFFERENTIATION

Monocytes and iDCs were defined by the expression of CD14 and CD1a, respectively [Chapuis et al., 1997]. PBMC were obtained from healthy adult volunteer donors. Informed consent was obtained from them. The ethics committee, Jichi Medical University School of Medicine approved this study. A positive selection of $CD14^+$ cells was performed by adding MACS colloidal superparamagnetic microbeads conjugated with monoclonal anti-human CD14 Abs (IgG2a), (Miltenyi Biotec, Tokyo, Japan) to freshly prepared PBMC preparation in MACS buffer according to the manufacture′s instructions. Briefly, after incubation of cells and microbeads (15 min at 4°C), cells were washed with MACS buffer, resuspended, and loaded onto the top of the separation column. Trapped $CD14^+$ PBMC were eluted with a sixfold amount of cold MACS buffer. Using flow cytometry, the purity of the $CD14^+$ cells was evaluated at $98.8 \pm 0.4\%$.

Purified monocytes were used to generate monocyte-derived iDCs in vitro, as previously described [Rivollier et al., 2004]. Briefly, monocytes were seeded at 10^6 cells/ml and maintained in RPMI 1640 (Life Technologies, Paisley, UK) supplemented with 10 mM N-2-hydroxyethylpiperazine-N′-2-ethanesulfonic acid (HEPES), 2 mM L-glutamine, 100 U/ml penicillin and 100 μg/ml streptomycin (Life Technologies), 10% heat-inactivated fetal calf serum (FCS; Biological Industries, Beit Haemek, Israel), 50 ng/ml human recombinant (h) granulocyte-macrophage colony-stimulating factor (GM-CSF), and 500 U/ml h IL-4 (PeproTech, Rocky Hill, NJ). After 5 days in culture, more than 90% of the cells were iDCs as assessed by CD1a labeling.

OC-LIKE MGC FORMATION AND TRAP ASSAY

iDCs were seeded at 1,600 cells/mm^2 in 48-well plates, into which a sterilized glass coverslip was placed, in α-minimum essential medium (α-MEM) (Life Technologies) supplemented with 10% FCS, 2 mM L-glutamine, 100 U/ml penicillin, and 100 μg/ml streptomycin in the presence of 25 ng/ml M-CSF and 100 ng/ml RANKL (PeproTech, Rocky Hill, NJ). During the course of differentiation, we harvested culture supernatants and various cells including monocytes, iDCs, and various differential stages of OC-like MGCs at day 4 (OC4), day 8 (OC8), and day 12 (OC12). Tartrate-resistant acid phosphatase (TRAP) activity, a signature marker for OCs, was assessed using a leukocyte acid phosphatase kit (Sigma–Aldrich) at day 12. Nuclear DNA was stained with 10 μg/ml Hoechst 33342 (Sigma–Aldrich) for 30 min at 37°C and fixed with 15% formol.

SUPPRESSION OF OPN BY RNA INTERFERENCE

Suppression of OPN expression was performed by RNA interference using specific small interfering RNA oligonucleotides (siRNA) (ccaaguaaguccaacgaaaTT). Control siRNA sequence was acucuaucugcacgcugacTT. siRNAs were transfected into human monocytes or monocyte-derived iDCs using Lipofectamine RNAiMAX (Life Technologies). Transfected monocytes or iDCs were cultured to form OC-like MGCs as described above. The number of OC-like MGCs (TRAP-positive and strictly more than two nuclei) was counted on day 7 of OC differentiation.

INHIBITION OF MGC FORMATION WITH SYNTHETIC PEPTIDES DERIVED OPN INTERNAL SEQUENCE

In order to examine whether the interaction of OPN and its receptors is involved in MGC formation, we used synthetic peptides (RGD and SVVYGLR) to both RGD-recognizing and SVVYGLR-recognizing integrins. RGD and SVVYGLR peptides interfere with the binding of OPN to RGD- and non RGD ($\alpha4\beta1$ and $\alpha9\beta1$) integrins, respectively [Storgard et al., 1999; Green et al., 2001]. MGCs were differentiated from iDCs, in the presence of 10 μg/ml RGD or RGE (control) peptides (Abbiotec, San Diego, CA), or 1 μg/ml SVVYGLR or GRVLYSV (control) peptides (GenScript, Piscataway, NJ). The number of OC-like MGCs (TRAP-positive and strictly more than two nuclei) was counted on day 7 of OC differentiation.

IMMUNOFLUORESCENCE AND MICROSCOPY

Monocytes and iDC were attached to slide glass by cytospin. Monocytes, iDC and cells cultured on glass coverslips (OC4, OC8, OC12) were first fixed with 4% paraformaldehyde for 30 min at 4°C. The slide glass or the glass coverslips were incubated in normal goat serum for 30 min at 30°C, followed by primary antibody (polyclonal rabbit anti-human OPN antibody (IgG), (Abcam, Cambridge, UK), polyclonal rabbit anti-human CD1a antibody (Sigma–Aldrich, St. Louis, MO), monoclonal mouse anti-human CD44v6 antibody (IgG1), (Leica, Newcastle upon Tyne, UK), monoclonal mouse anti-human $\alpha v\beta3$ antibody (IgG1), (Hycult Biotech, Uden, The Netherlands), and monoclonal mouse anti-human $\alpha9\beta1$ antibody (IgG1), (Abcam) for a further overnight at room temperature. Rabbit IgG (SP137), (Abcam) and mouse IgG1 (MOPC21), (Affinity BioReagents, Golden, CO) was used as substitute isotype control. After washing with PBS, the appropriate secondary antibody (Alexa Fluor 488 goat anti-mouse IgG (H + L), Alexa Fluor 488 goat anti-rabbit IgG (H + L), or Alexa Fluor 555 goat anti-mouse IgG (H + L) (Molecular Probes, Inc., Eugene, OR) was applied for 30 min at 30°C. Nuclear DNA was stained by DAPI (4′-6-diamidino-2-phenylindole). The cells were analyzed using an Olympus AX80 microscope equipped with an 40×/0.85 NA or a 100×/1.35 oil iris NA objective lens, an Olympus DP70 camera, and Olympus DP controller software (Olympus Co. Ltd., Tokyo, Japan). The number of CD1a positive cells and $\alpha9\beta1$ positive cells was counted on monocyte, iDC, and day 4, 8, 12 of OC differentiation.

QUANTIFICATION OF IMMUNOFLUORESCENCE

Images collected using the Olympus DP controller software were analyzed for immunofluorescence intensity using Adobe Photoshop Elements, version 11 (Adobe Systems Incorporated, Tokyo, Japan) as follows. Using the magic wand tool in the "Select" menu of Photoshop, the cursor was placed on α9β1-positive cytoplasm. The tolerance level of the magic wand tool was adjusted so that the entire positive cytoplasm was selected automatically. The mean staining intensity was calculated as follows: intensity score (IS) = mean of brightness of selected cells' red channel score (in arbitrary units, AU) using Adobe Photoshop Elements, version 11 [Murakami et al., 2013].

RELATIVE QUANTITATIVE RT-PCR

Levels of OPN, CD44v6, integrin αv, and integrin α9 mRNA were measured by relative quantitative real-time reverse transcription polymerase chain reaction (RT-PCR) using the 7500 Fast System (Applied Biosystems, Foster City, CA); β-actin was used as an internal standard. Briefly, RNA was isolated from the harvested cells using an RNeasy kit (Qiagen, Hilden, Germany), reverse transcribed, and PCR amplified using a One Step PrimeScript RT-PCR Kit (Takara Bio, Shiga, Japan), with TaqMan Gene Expression Assay primers for human OPN (Hs00959010), integrin αv (Hs00233808), integrin α9 (Hs00979865), CD44v6 (Hs01075854), and β-actin (Hs99999903). Data were analyzed using the $2^{-\Delta\Delta C_t}$ method.

MEASUREMENTS OF THE FULL-LENGTH AND THE CLEAVED FORMS OF OPN IN THE CELL SUPERNATANT

We measured the amounts of the full-length OPN in the cell culture supernatant with human osteopontin ELISA kit (R&D Systems, Minneapolis, MN) and the cleaved forms of OPN with human osteopontin N-half assay kit (IBL, Gunma, Japan), which can specifically measure the N-terminal OPN fragment cleaved by thrombin. N-terminal OPN fragments expose a cryptic epitope, SVVYGLR, which is recognized by α9β1 integrin. Thus, the presence of high amounts of N-half OPN indicates the involvement of α9β1 integrin in OC-like MGC differentiation.

FLOW CYTOMETRIC ANALYSIS

We used directly conjugated antibodies, FITC-anti-CD14 (M5E2), PE-anti-CD1a (HI149), FITC-IgG2a (G155-178), and PE-IgG1 (MOPC-21) (BD Pharmingen, Tokyo, Japan). Cells were suspended in PBS supplemented with 10% FCS (FACS buffer) and stained with appropriate concentrations of antibodies for 15 min on ice, then washed with FACS buffer. Cells were analyzed using a BD LSR cytometer and CellQuest software (BD, Tokyo, Japan).

DETERMINATION OF VIABILITY AND APOPTOSIS

For floating cells, we analyzed the proportion of viable and apoptotic cells using flow cytometry. The number of floating cells was counted, cells were suspended in binding buffer (BD Pharmingen, Tokyo, Japan), and cell suspensions were incubated with Annexin V-PE and 7-AAD (BD Pharmingen, Tokyo, Japan) for 15 min at room temperature. Cells were analyzed using a BD LSR Fortessa cell analyzer and FlowJo software (Tree Star, San Carlos, CA). Unstained cells were used as negative controls. Viable cells were defined as double negative for Annexin V and 7-AAD, and apoptotic cells were defined as Annexin V positive and 7-AAD negative. For analysis of adherent cells, cells cultured on glass coverslips were stained by 0.4% trypan blue to count viable cells. To detect apoptotic cells, terminal deoxynucleotidyl transferase mediated dUTP nick end labeling (TUNEL) stain was performed. Cells were fixed with 4% paraformaldehyde for 30 min at 4°C. The glass coverslips were incubated with permeabilization buffer for 2 min at 4°C, followed by FITC-labeled terminal deoxynucleotidyl transferase (TdT) enzyme for 90 min at 37°C. DNA was stained by DAPI. The cells were analyzed using an Olympus AX80 microscope.

QUANTIFICATION OF CASPASE-3 ACTIVITY

Caspase-3 activity was quantified using an ApoAlert Caspase-3 colorimetric assay kit (Clontech, Tokyo, Japan). This assay uses the spectrophotometric detection of the chromophore p-nitroaniline (pNA) after its cleavage by caspases from the labeled caspase-specific substrates. 1.5×10^5 cells were harvested at each stage (OC1, OC3, and OC7), and resuspended in 50 μl of lysis buffer and incubated for 10 min at 4°C. Cell suspension were centrifuged at 15,000 rpm for 10 min. Twenty-five microliters of the supernatants were added to 25 μl of 2× reaction buffer, and then incubated with caspase-3 substrate, aspartic acid-glutamic acid-valine-aspartic acid (DEVD)-p-nitroaniline (pNA), for 60 min at 37°C. The chromophore pNA was measured at 405 nm in Benchmark Plus microplate reader (BIO-RAD, Tokyo, Japan). We constructed a standard curve for each assay run using pNA in the concentration range of 0–200 μM, and converted optical density of each sample into pNA concentration.

MEASUREMENT OF INTRACELLULAR REACTIVE OXYGEN SPECIES PRODUCTION

Reactive oxygen species (ROS) activity was quantified using an OxiSelect Intracellular ROS assay kit (Cell Biolabs, San Diego, CA). Briefly, 1.5×10^5 cells were harvested at each differentiation stage (Mo, iDC, OC1, OC3, and OC7), and then incubated with 100 μl of 2′, 7′-dichlorodihydrofluorescin diacetate (DCFH-DA) at 37°C for 60 min. Cells were washed twice with PBS, and lysed by cell lysis buffer. Fluorescence was measured at 480 nm excitation/530 nm emission in Wallac 1420 ARVO MX (Perkin Elmer, Yokohama, Japan). We constructed a standard curve for each assay run using 2′, 7′-dichlorodihydrofluorescein (DCF) in the concentration range of 0–10 μM, and converted fluorescence intensity into DCF concentration.

INHIBITION OF ROS GENERATION

We used diphenyleneiodonium chloride (DPI) (Enzo Life Sciences, Lausen, Switzerland) or *N*-acetyl-L-cysteine (NAC) (Sigma–Aldrich) as ROS inhibitors. DPI was dissolved in Dimethyl sulfoxide (DMSO). NAC was dissolved in α-MEM, and pH was adjusted to 7.4 by the addition of NaOH. Monocytes or iDCs were incubated with 100 nM DPI or 20 mM NAC for 60 min at 37°C, and washed twice with medium. Pretreated monocytes were cultured with GM-CSF and IL-4 for 5 days, and pretreated iDCs were cultured with M-CSF and RANKL for 7 days.

STATISTICAL ANALYSIS

The paired *t*-test was used to analyze the difference between groups; $P < 0.05$ was considered significant. All error bars in this study represent the standard error mean of the mean (SEM). Statistical analyses were performed using Microsoft Excel software.

RESULTS

OPN PRODUCTION IS INCREASED DURING THE COURSE OF OC-LIKE MGC FORMATION FROM iDCs

The production of OPN mRNA and protein was investigated over the course of OC-like MGC formation from iDCs in vitro. First, we obtained monocytes from the blood of healthy adult volunteer donors and from them generated iDCs and then OC-like MGCs using an in vitro culture system (Fig. 1A). During the course of differentiation, we harvested culture supernatants and various cells including monocytes, iDCs, and various differential stages of OC-like MGCs at day 4 (OC4), day 8 (OC8), and day 12 (OC12). Monocytes had no detectable

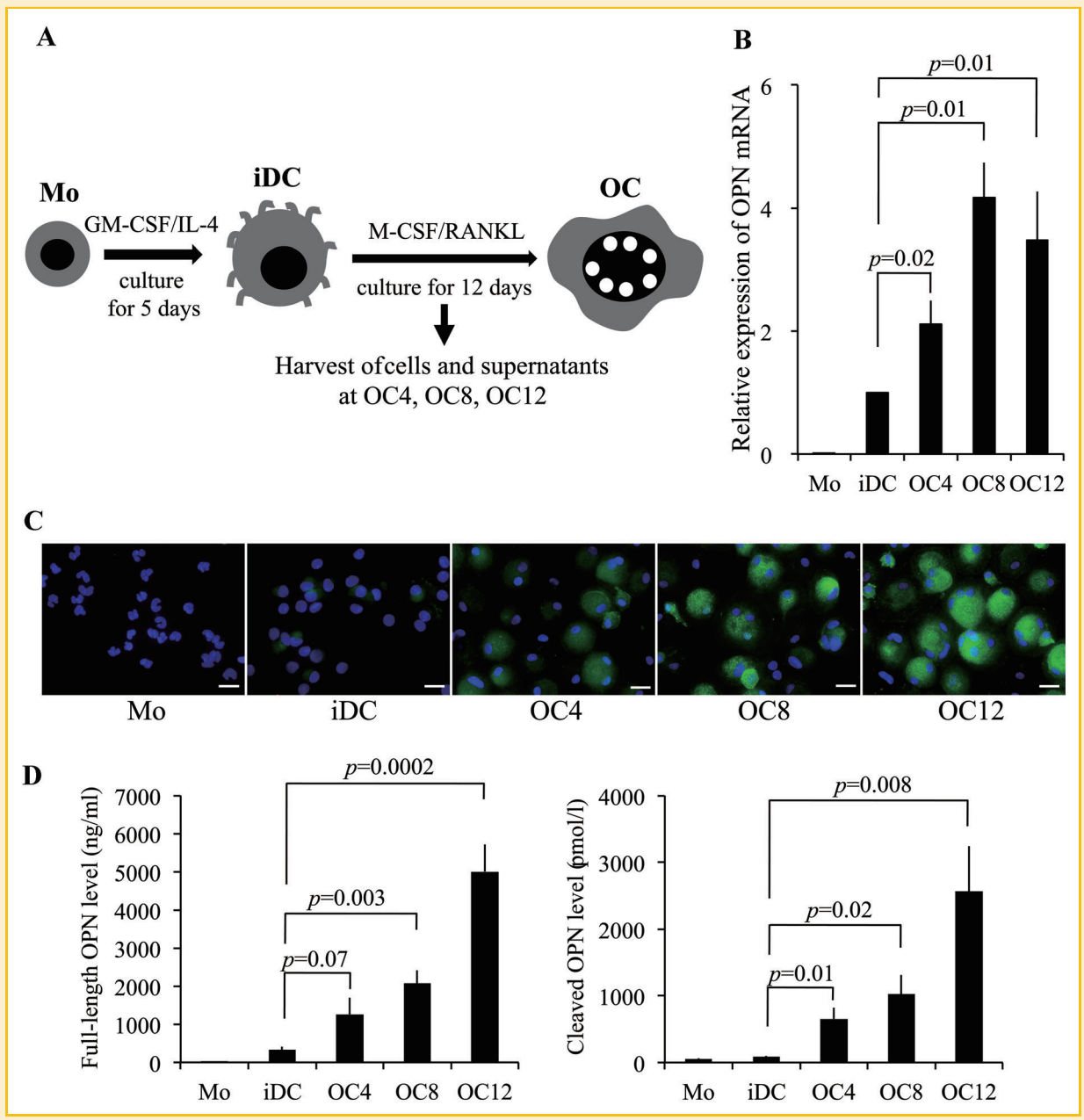

Fig. 1. OPN production in the course of OC-like MGC formation from iDCs in vitro. A: Schema of experimental design. Monocytes were purified from the peripheral blood of healthy adult volunteer donors. Monocyte-derived immature dendritic cells were generated in vitro by culturing for 5 days with GM-CSF/IL-4. Osteoclasts were generated in vitro by culturing iDCs for 12 days with M-CSF/RANKL. Cells and supernatants were harvested from the starting population of monocytes, the resultant iDCs, and OC-like MGCs on day 4, day 8, and day 12 of culture. B: OPN mRNA expression measured by relative quantitative RT-PCR (data shown are the mean of experiments with cells from five donors). Error bars represent mean ± SEM. C: Immunofluorescence staining with anti-OPN antibody (green) and DAPI (blue) performed on Mo, iDC, OC4, OC8, and OC12. Bars: 20 μm. D: Full-length and cleaved OPN in the cell culture supernatants of OC differentiation from iDCs (independent experiments with cells from eight donors). Error bars represent mean of the eight experiments ± SEM. GM-CSF, granulocyte-macrophage colony-stimulating factor; iDC, immature dendritic cell; M-CSF, macrophage colony-stimulating factor; MGC, multinucleated giant cell; Mo, monocyte; OC: osteoclast; OC4, OC-like MGCs on day 4; OC8, OC-like MGCs on day 8; OC12, OC-like MGCs on day 12; OPN, osteopontin; RANKL, receptor activator of NF-κB ligand; siRNA, small interfering RNA.

OPN mRNA, but the level expressed by iDCs was exceeded by differentiation stage OC8 (Fig. 1B). To characterize the OPN-producing cells further, we performed immunofluorescence staining on samples of each cell population (monocytes, iDCs, OC4, OC8, and OC12). Monocytes and iDC were attached to slide glass by cytospin. OC4, OC8, and OC12 were cultured on glass coverslips. In accordance with the increase in OPN mRNA expression found over the course of culture, production of OPN increased with differentiation: monocytes did not produce OPN, iDCs started to produce relatively small amounts, and OC12 produced the highest levels of OPN (Fig. 1C). The concentration of both the full-length and the cleaved forms of OPN in the cell supernatant steadily increased during the course of OC-like MGC formation (Fig. 1D).

EXPRESSION OF OPN RECEPTORS DURING THE COURSE OF OC-LIKE MGC GENERATION FROM iDCs

Next, we investigated the expression of receptors for OPN, specifically αvβ3 integrin, CD44v6, and α9β1 integrin, during the course of OC-like MGC formation. The mRNA levels of αvβ3 integrin, CD44v6, and α9β1 integrin increased and peaked at OC8 or OC12 (Fig. 2A), following a similar pattern to OPN production. CD44v6 mRNA was highly expressed by monocytes; however, its expression by iDCs was low. To characterize OPN receptor-expressing cells further we examined αvβ3-, CD44v6-, and α9β1-expressing OC12 for TRAP and OPN expression using immunofluorescence staining. Furthermore, to know whether iDCs remain at the end of culture, OC12, and whether the remaining iDCs are involved in the formation of OC-like

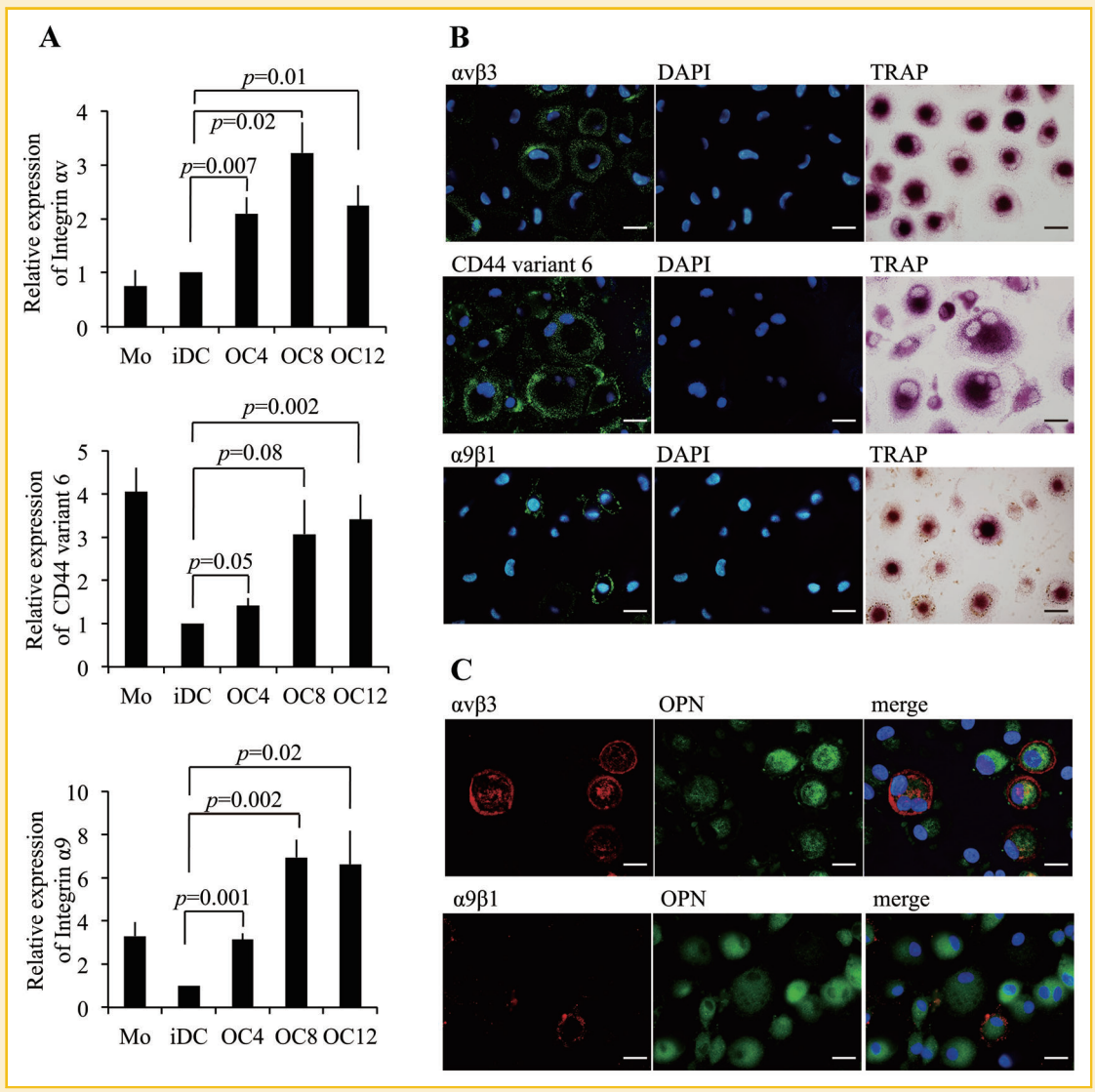

Fig. 2. OPN receptor expression during the course of OC-like MGC formation from iDCs and characterization of αvβ3-, CD44v6-, and α9β1-expressing cells. A: Expression of integrin αv mRNA (receptor for full-length OPN), CD44v6 mRNA (receptor for full-length OPN), and integrin α9 mRNA (receptor for cleaved OPN) measured by relative quantitative RT-PCR (data shown are the mean of experiments with cells from five donors). Error bars represent mean ± SEM. B: Detection of αvβ3, CD44v6 (receptors for full-length OPN), and α9β1 (receptor for cleaved OPN) by immunofluorescence staining (green) of OC12. Nuclei were stained with DAPI (blue). TRAP activity was assessed on the same glass coverslips. Bars: 20 μm. Data shown are representative of ten experiments. C: Detection of OPN (green) and its receptor (red) by double immunofluorescence staining. Nuclei were stained with DAPI (blue). Bars: 20 μm. Data shown are representative of 10 experiments. DAPI, 4′,6-diamidino-2-phenylindole; TRAP, tartrate-resistant acid phosphatase.

MGCs, we stained iDC marker, CD1a. Cells expressing αvβ3 were both TRAP- and OPN-positive but CD1a-negative, and some were multinucleated but with no more than four nuclei (Figs. 2B,C and 3A), suggesting that they were not fully mature OC-like MGCs. CD44v6-expressing cells were also TRAP-positive, and most were typical MGCs (Fig. 2B), suggesting that they were mature OC-like MGCs. On the other hand, α9β1-expressing cells were both OPN- and CD1a-positive but TRAP-negative with a single nucleus, and some were spindle shaped with processes characteristic of iDCs (Figs. 2B,C and 3A). Using fluorescence intensity scoring, we showed that cells expressing α9β1 existed before the start of OC differentiation and some iDCs expressed α9β1 integrin weakly but, while its expression became stronger during the course of OC-like MGC formation (Fig. 3B, Supplementary Fig. S1). The number of α9β1- and CD1a-positive cells did not increase (Fig. 3C,D). These data indicate that some remaining iDCs express α9β1 integrin strongly instead of the increased number of α9β1-positive cells. This suggests that α9β1- and CD1a-positive cells might have some role in OC-like MGCs formation.

OC-LIKE MGC FORMATION IS SUPPRESSED BY DOWN-REGULATION OF OPN

To study the role of OPN in OC-like MGC formation, we down-regulated the expression of OPN by transfection with OPN siRNA at the initial monocyte stage, or at the iDC stage (Fig. 4A). First, we generated iDCs from monocytes that had been transfected with either OPN siRNA or control siRNA. There was no difference in efficacy of differentiation of monocytes into iDCs between monocytes transfected with OPN siRNA or control siRNA, as judged by the expression of CD1a (Supplementary Fig. S2). Next, we prepared two types of iDCs, one derived from monocytes that had been treated with OPN

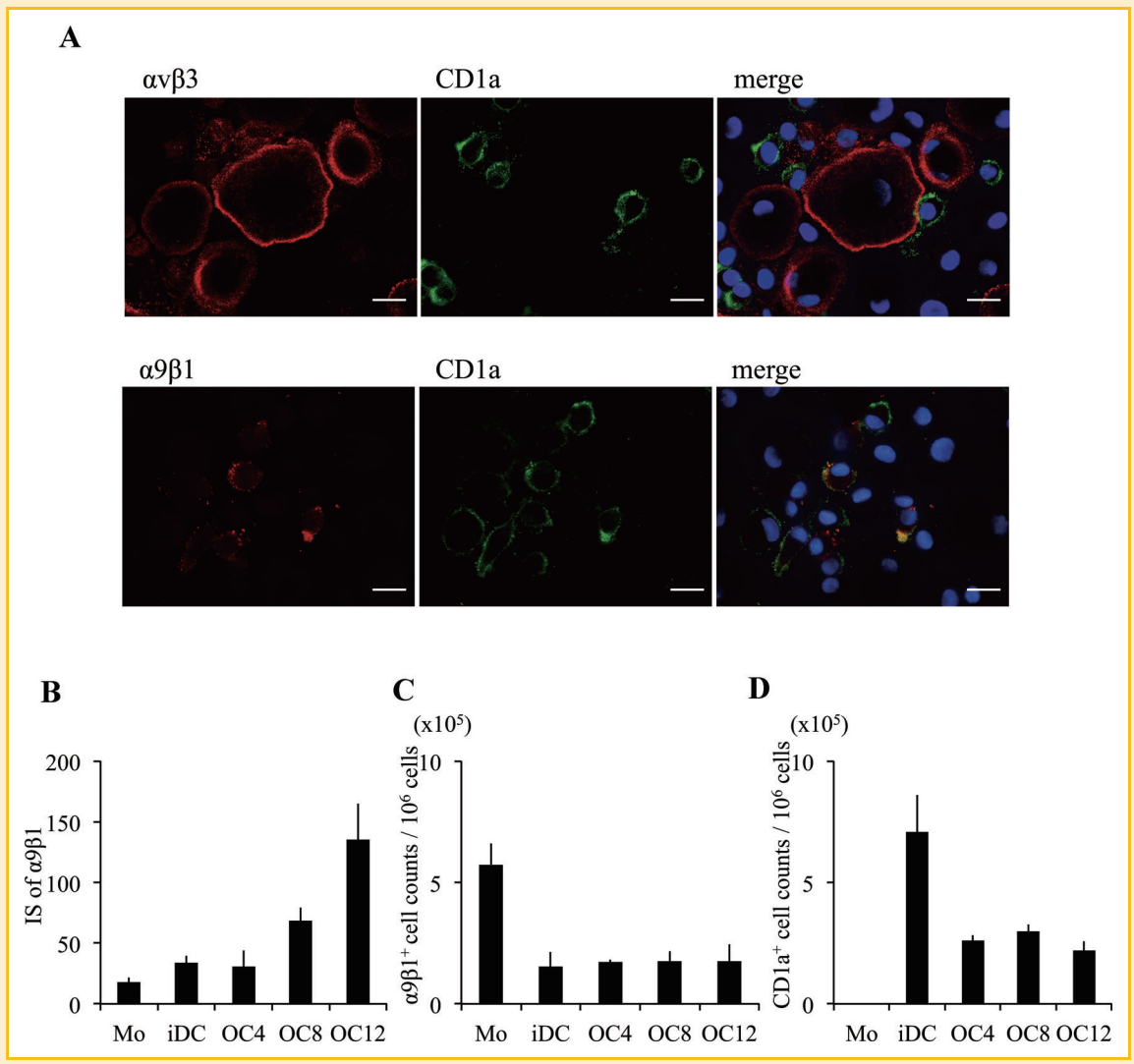

Fig. 3. The relationship between OPN receptors and CD1a. A: Detection of CD1a (green) and OPN receptors (red) by double immunofluorescence staining, Nuclei were stained with DAPI (blue). Bars: 20 μm. Data shown are representative of 10 experiments. B: Immunofluorescence data providing the IS of α9β1 expressed. The mean staining intensity was calculated as follows: IS, mean of brightness of selected cells' red channel score (in arbitrary units, AU) using Adobe Photoshop Elements, version 11. Data shown are the mean of experiments with cells from three donors. Error bars represent mean ± SEM. C: Number of α9β1-positive cells per 1×10^6 cells (data shown are the mean of experiments with cells from three donors). D: Number of CD1a-positive cells per 1×10^6 cells (data shown are the mean of experiments with cells from three donors). IS, intensity score.

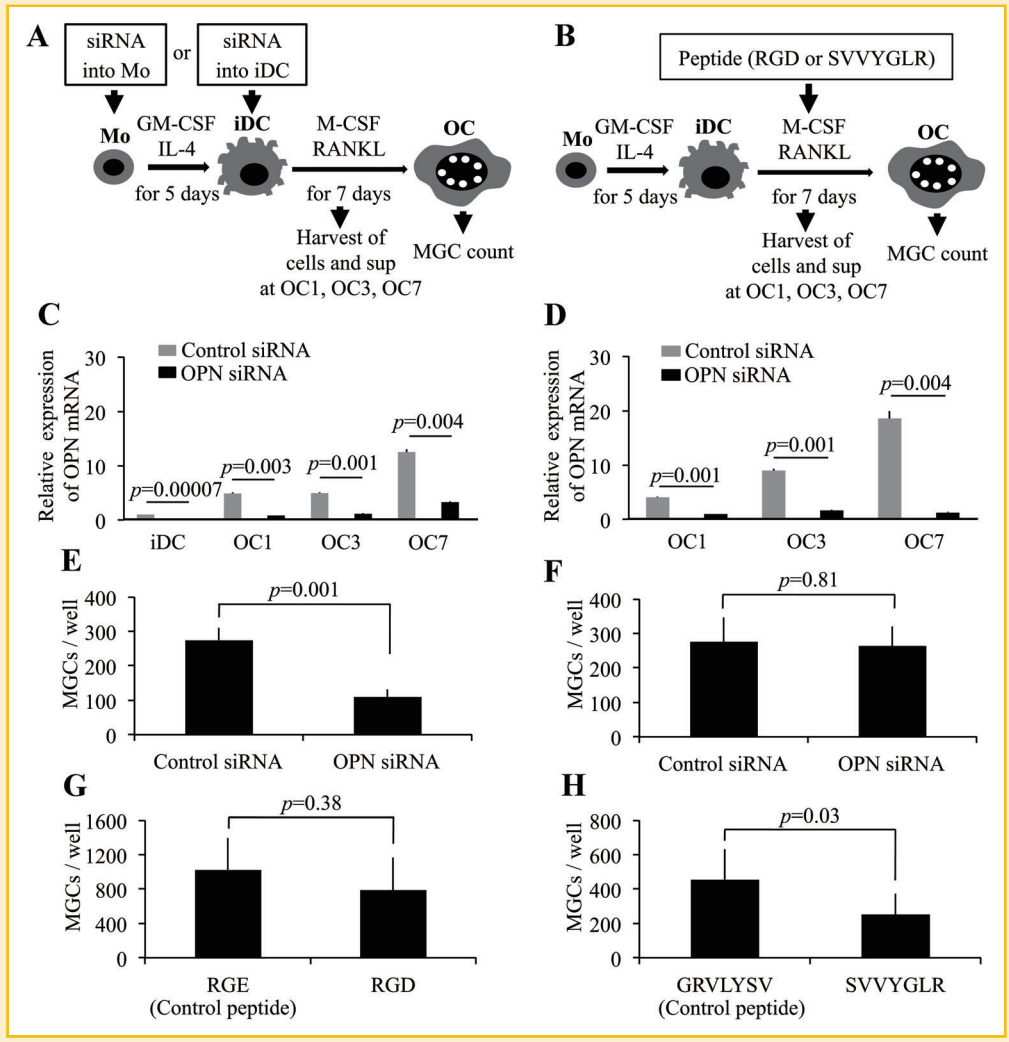

Fig. 4. The effect on MGC formation from iDC of down-regulating OPN with siRNA and inhibiting OPN binding. A: To study the role of OPN on OC-like MGC generation, OPN expression was down-regulated by transfection of OPN siRNA into monocytes or iDCs derived from non-treated monocytes. B: To identify the type of OPN receptor involved in MGC generation, two different synthetic peptides, RGD or SVVYGLR, were included in the culture medium during the differentiation of iDCs into OC-like MGCs. C, D: OPN mRNA levels measured by relative quantitative RT-PCR in OC-like MGC generated from (C) siRNA-transfected monocytes (data shown are the mean of experiments with cells from ten donors) or (D) siRNA-transfected iDCs (data shown are the mean of experiments with cells from ten donors). E, F: Number of MGCs differentiated from (E) iDCs generated from siRNA-transfected monocytes (data shown are the mean of experiments with cells from ten donors) or (F) siRNA-transfected iDCs (data shown are the mean of experiments with cells from ten donors). The number of MGCs was counted at OC7. G: Number of MGCs differentiated from iDCs in the presence of 10 μg/ml RGE (control) or RGD peptides (data shown are the mean of experiments with cells from five donors). H: Number of MGCs differentiated from iDCs in the presence of 1 μg/ml GRVLYSV (control) or SVVYGLR peptides (data shown are the mean of experiments with cells from six donors). MGCs were counted at OC7. Error bars represent mean $\pm$ SEM. OC1, OC-like MGCs on day 1; OC3, OC-like MGCs on day 3; OC7, OC-like MGCs on day 7; sup, supernatants.

siRNA (Fig. 4C,E), and the other derived from non-treated monocytes, which were treated with OPN siRNA at the iDC stage (Fig. 4D,F). Subsequently both types of iDCs were cultured for a further 7 days. Cells and supernatants were recovered at day 1, 3, and 7 and thus these cells were referred to as OC1, OC3, and OC7, respectively. The numbers of OC-like MGCs were counted on day 7 (OC7). With the exception of OC1, the concentration of full-length and cleaved forms of OPN in the supernatant of cells differentiated from both types of iDCs was reduced in OPN siRNA-transfected cells compared to cells transfected with control siRNA (Supplementary Fig. S3). Nevertheless, OPN mRNA expression was efficiently reduced by OPN siRNA treatment (Fig. 4C,D). By the end of culture on day 7, there was a significant reduction in MGC formation by iDCs derived from monocytes treated with OPN siRNA (Fig. 4E), while OPN siRNA-treated iDCs derived from non-treated monocytes were able to generate MGCs (Fig. 4F). These data suggest that OPN plays a role in the early phase of OC and/or MGC differentiation, specifically during the differentiation of monocytes to iDCs.

MGC FORMATION IS REDUCED BY SVVYGLR PEPTIDES

To investigate the type of OPN receptor involved in MGC formation, we used two different synthetic peptides, corresponding to internal

sequences of OPN, namely RGD, which binds RGD-recognizing integrins including αvβ3 and α5β1, and SVVYGLR, which is recognized by α4β1 and α9β1. These peptides were added to the culture medium during the differentiation of iDCs into OC-like MGCs (Fig. 4B). No obvious effect on MGC formation by RGD peptide compared to the RGE control peptide was observed (Fig. 4G). However, MGC formation was significantly reduced by SVVYGLR peptide as compared to the GRVLYSV control peptide (Fig. 4H), suggesting that α4β1 and/or α9β1 integrin receptors play a pivotal role in MGC formation.

OPN DID NOT AFFECT VIABILITY AND APOPTOSIS IN OC-LIKE MGC FORMATION

OPN is known to confer resistance to apoptosis [Tuck et al., 2007; Yamaguchi et al., 2013]. In inflammatory bone diseases, osteolytic lesions can be treated with bisphosphonates [Morimoto et al., 2011], which induce OC apoptosis [Abe et al., 2012]. Based on these reports, we hypothesized that OPN promote the survival and inhibit the apoptosis of OC precursor cells or OCs, consequently OC-like MGC formation is increased. We evaluated whether OPN affects cell viability and apoptosis in the course of OC-like MGC formation, using OPN siRNA-transfected or control siRNA-transfected monocyte-derived iDC. We determined cell viability and apoptosis by flow cytometry for floating cell and trypan blue stain and TUNEL stain for tightly adhering cells. Additionally, we performed Caspase-3 activity assay. Caspase-3 is an active cell-death protease involved in the execution phase of apoptosis, where cells undergo morphological changes such as DNA fragmentation, chromatin condensation, and apoptotic body formation [Porter and Janicke, 1999]. The number of viable cell and apoptotic cell, and caspase-3 activity were not affected by down-regulation of OPN (Fig. 5A–C).

OXIDATIVE STRESS IS NOT INVOLVED IN OPN PRODUCTION DURING THE COURSE OF OC-LIKE MGC FORMATION

In view of previous reports demonstrating that reactive oxygen species (ROS) may play a significant role as second messengers for the expression of osteopontin in mice [Umekawa et al., 2009; Lyle et al., 2012], it is an interesting issue whether ROS is linked to OPN production in human primary cells. To answer this question, we examined intracellular ROS activity and OPN production with or without ROS inhibitor of diphenyleneiodonium chloride (DPI) or *N*-acetyl-L-cysteine (NAC) in our culture system. DPI is a competitive inhibitor of flavin-containing cofactors and a very potent inhibitor of NADPH oxidase [Hancock and Jones, 1987]. NAC, in contrast, acts as a scavenger of ROS regardless of the source of production [Aruoma et al., 1989]. ROS was already generated at the differentiation into iDCs from monocytes, and came up to the highest levels at OC7 (Fig. 6A). As previous research has indicated [Del Prete et al., 2008], iDC differentiation from monocyte was suppressed when monocytes were pretreated with ROS inhibitor (Supplementary Fig. S4). We next treated iDCs with a non-cytotoxic concentration of DPI (100 nM) or NAC (20 mM), and evaluated the effect of ROS inhibitors on OPN production. Although ROS activity was significantly suppressed at OC7 (Fig. 6B), OPN production was not decreased (Fig. 6C,D). Because OPN is also known to reduce intracellular ROS during hypoxia/reperfusion to protect cells from oxidative injury [Denhardt et al., 1995], we examined intracellular ROS activity with or without down-regulation of OPN during the course of OC-like MGC formation. The down-regulation of OPN did not affect intracellular ROS activity (Supplementary Fig. S5).

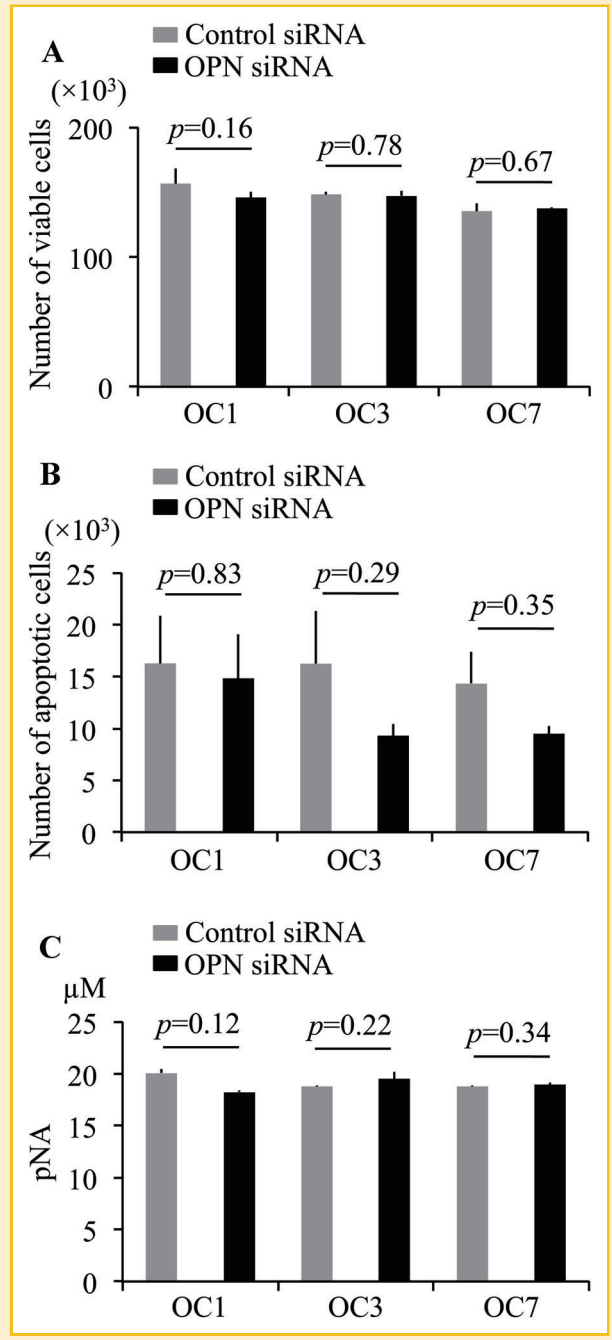

Fig. 5. Viability and apoptosis in the course of OC-like MGC differentiation from iDC of down-regulating OPN with siRNA. A: Number of viable cells. B: Number of apoptotic cells. C: Quantification of caspase-3 activity. We detected pNA as cleavage product by caspase-3. Data shown are the mean of experiments with cells from four donors. Error bars represent mean ± SEM. pNA, p-nitroaniline.

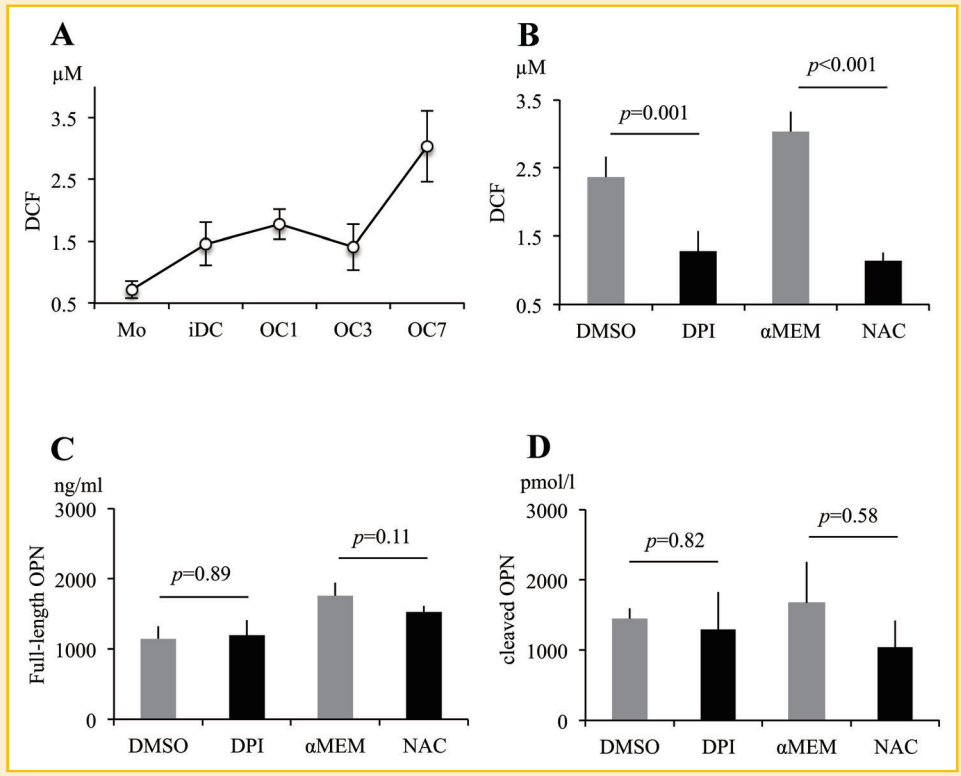

Fig. 6. The relation between ROS activity and OPN production. A: ROS activity during the course of MGC formation. We detected DCF as oxidized product by intracellular ROS. B: The effect of ROS inhibitor at OC7. C: Full-length OPN in the supernatants at OC7 differentiated from DPI- or NAC-treated iDC. D: Cleaved OPN in the supernatants at OC7 differentiated from DPI- or NAC-treated iDC. Data shown are the mean of experiments with cells from four donors. Error bars represent mean ± SEM. DCF, 2′, 7′-dichlorodihydrofluorescein; α-MEM, α-minimum essential medium; DMSO, Dimethyl sulfoxide; DPI, diphenyleneiodonium chloride; NAC, N-acetyl-L-cysteine.

DISCUSSION

In this study, we found that during the course of OC-like MGC formation from iDC, a large amount of OPN (both mRNA and protein) was produced, the cultured cells expressed OPN receptors, and inhibiting OPN expression suppressed OC-like MGC formation. These results indicate that OPN plays an important role in OC-like MGC formation from iDCs.

All cells expressed OPN during the course of OC-like MGC formation from iDCs in vitro. On the other hand, OPN receptors that recognize full-length OPN were expressed on TRAP-positive and CD1a-negative multinucleated cells, while the α9β1 integrin receptor, which recognizes the cleaved form of OPN, was expressed on TRAP-negative and CD1a-positive mononuclear cells. This indicates that full-length OPN stimulates cells that have differentiated into OC-like MGCs, while the cleaved form of OPN stimulates cells that have retained the character of iDCs. MGC formation from iDCs transfected with OPN siRNA was not suppressed, but that from iDCs generated from OPN-transfected monocytes was significantly suppressed. The differentiation of monocytes into iDCs was not itself influenced by OPN suppression. This indicates that OPN is crucial for OC-like MGC formation during the early phase, although OPN levels in OC1 cell culture supernatants were not significantly different between OPN siRNA- and control siRNA-transfected cells. There is a possibility that a critical OPN level for iDC fusion and OC-like MGC formation exists in the early phase of culture. MGC formation was not suppressed by the RGD peptide, which interferes with the interaction of full-length OPN with its receptor, but was significantly suppressed by SVVYGLR peptide, which interferes with the interaction of the cleaved form of OPN with its receptor. These findings suggest that cleaved OPN has a key role in stimulating iDC to differentiate into OC-like MGCs in an autocrine manner.

OPN has been known as a multi-functional secreted phosphoglycoprotein, which is involved not only in bone resorption by OCs but also in the immune defense system and autoimmune disease. Recently, an increasing number of reports describe the association between OPN and the inflammatory bone disease of RA and LCH. In mouse models of collagen-induced arthritis, OPN deficiency prevents development of the disease [Yumoto et al., 2002] and anti-OPN antibody, which blocks the interaction of OPN with its integrins, significantly inhibits disease development [Yamamoto et al., 2007]. Bronchoalveolar lavage cells from patients with pulmonary LCH spontaneously produce abundant amounts of OPN and OPN overexpression in rat lungs induces lesions similar to pulmonary LCH, with marked alveolar and interstitial accumulation of Langerhans cells [Prasse et al., 2009]. Furthermore, OPN is highly overexpressed in T cells and LCH cells of the LCH lesion [Allen et al., 2010].

T cells and antigen-presenting cells, such as DCs and macrophages, secrete OPN causing autocrine or paracrine stimulation that results in the secretion of other pro-inflammatory cytokines. This pro-

inflammatory action is more strongly induced by cleaved than full-length OPN [Uede, 2011]. For example, it was reported that the production by vascular smooth-muscle cells of free radicals related to oxidative stress was greater in response to cleaved OPN than in response to full-length OPN [Lai et al., 2006]. The adhesive ability of the cleaved OPN is also enhanced in comparison to that of full-length OPN [Gao et al., 2004]. Cleaved OPN and its receptors (the $\alpha4\beta1$ and $\alpha9\beta1$ integrins) are involved in the neutrophil infiltration and hepatic injury in inflammatory liver diseases [Diao et al., 2004]. Additionally, the cleaved form of OPN plays a critical role in RA [Morimoto et al., 2010; Uede, 2011], while a role for the cleaved form of OPN in LCH has not been revealed. In this paper, we demonstrate the role of cleaved OPN in the formation of OC-like MGCs from iDCs. Cleaved OPN could therefore plausibly play a role in the pathogenesis of both RA and LCH in which OCs are intimately involved [Redlich et al., 2002; da Costa et al., 2005].

OPN did not affect viability and apoptosis in OC-like MGC formation, suggesting OPN directly acts as a signal mediator for OC-like MGC formation. ROS activity increased during OC-like MGC formation, however, we could not discover any relation between ROS activity and OPN production.

ACKNOWLEDGMENTS

This study was supported by a grant for Research on Measures for Intractable Diseases from the Ministry of Health, Labor and Welfare, Japan and Grant-in-Aid for Scientific Research (KAKENHI) from the Ministry of Education, Culture, Sports, Science and Technology, Japan. This study was carried out under the Joint Research Program of the Institute for Genetic Medicine, Hokkaido University, and with funds from the JKA Foundation raised through its promotion of KEIRIN RACE. We thank Dr. Hiroko Hayakawa, of JMU Core Center of Research Apparatus, for help with flow cytometry.

REFERENCES

Abe K, Yoshimura Y, Deyama Y, Kikuiri T, Hasegawa T, Tei K, Shinoda H, Suzuki K, Kitagawa Y. 2012. Effects of bisphosphonates on osteoclastogenesis in RAW264.7 cells. Int J Mol Med 29:1007–1015.

Allen CE, Li L, Peters TL, Leung HC, Yu A, Man TK, Gurusiddappa S, Phillips MT, Hicks MJ, Gaikwad A, Merad M, McClain KL. 2010. Cell-specific gene expression in Langerhans cell histiocytosis lesions reveals a distinct profile compared with epidermal Langerhans cells. J Immunol 184:4557–4567.

Aruoma OI, Halliwell B, Hoey BM, Butler J. 1989. The antioxidant action of N-acetylcysteine: Its reaction with hydrogen peroxide, hydroxyl radical, superoxide, and hypochlorous acid. Free Radic Biol Med 6:593–597.

Chapuis F, Rosenzwajg M, Yagello M, Ekman M, Biberfeld P, Gluckman JC. 1997. Differentiation of human dendritic cells from monocytes in vitro. Eur J Immunol 27:431–441.

Chellaiah MA, Kizer N, Biswas R, Alvarez U, Strauss-Schoenberger J, Rifas L, Rittling SR, Denhardt DT, Hruska KA. 2003. Osteopontin deficiency produces osteoclast dysfunction due to reduced CD44 surface expression. Mol Biol Cell 14:173–189.

da Costa CE, Annels NE, Faaij CM, Forsyth RG, Hogendoorn PC, Egeler RM. 2005. Presence of osteoclast-like multinucleated giant cells in the bone and nonostotic lesions of Langerhans cell histiocytosis. J Exp Med 201:687–693.

Del Prete A, Zaccagnino P, Di Paola M, Saltarella M, Oliveros Celis C, Nico B, Santoro G, Lorusso M. 2008. Role of mitochondria and reactive oxygen species in dendritic cell differentiation and functions. Free Radic Biol Med 1:1443–1451.

Denhardt DT, Lopez CA, Rollo EE, Hwang SM, An XR, Walther SE. 1995. Osteopontin-induced modifications of cellular functions. Ann NY Acad Sci 760:127–142.

Diao H, Kon S, Iwabuchi K, Kimura C, Morimoto J, Ito D, Segawa T, Maeda M, Hamuro J, Nakayama T, Taniguchi M, Yagita H, Van Kaer L, Onóe K, Denhardt D, Rittling S, Uede T. 2004. Osteopontin as a mediator of NKT cell function in T cell-mediated liver diseases. Immunity 21:539–550.

Gao C, Guo H, Downey L, Marroquin C, Wei J, Kuo PC. 2003. Osteopontin-dependent CD44v6 expression and cell adhesion in HepG2 cells. Carcinogenesis 24:1871–1878.

Gao YA, Agnihotri R, Vary CP, Liaw L. 2004. Expression and characterization of recombinant osteopontin peptides representing matrix metalloproteinase proteolytic fragments. Matrix Biol 23:457–466.

Green PM, Ludbrook SB, Miller DD, Horgan CM, Barry ST. 2001. Structural elements of the osteopontin SVVYGLR motif important for the interaction with alpha(4) integrins. FEBS Lett 503:75–79.

Hancock JT, Jones OT. 1987. The inhibition by diphenyleneiodonium and its analogues of superoxide generation by macrophages. Biochem J 242:103–107.

Hu DD, Lin EC, Kovach NL, Hoyer JR, Smith JW. 1995. A biochemical characterization of the binding of osteopontin to integrins alpha v beta 1 and alpha v beta 5. J Biol Chem 270:26232–26238.

Lai CF, Seshadri V, Huang K, Shao JS, Cai J, Vattikuti R, Schumacher A, Loewy AP, Denhardt DT, Rittling SR, Towler DA. 2006. An osteopontin-NADPH oxidase signaling cascade promotes pro-matrix metalloproteinase 9 activation in aortic mesenchymal cells. Circ Res 98:1479–1489.

Lyle AN, Joseph G, Fan AE, Weiss D, Landázuri N, Taylor WR. 2012. Reactive oxygen species regulate osteopontin expression in a murine model of postischemic neovascularization. Arterioscler Thromb Vasc Biol 32:1383–1391.

Morimoto A, Shioda Y, Imamura T, Kanegane H, Sato T, Kudo K, Nakagawa S, Nakadate H, Tauchi H, Hama A, Yasui M, Nagatoshi Y, Kinoshita A, Miyaji R, Anan T, Yabe M, Kamizono J. 2011. Nationwide survey of bisphosphonate therapy for children with reactivated Langerhans cell histiocytosis in Japan. Pediatr Blood Cancer 56:110–115.

Morimoto J, Kon S, Matsui Y, Uede T. 2010. Osteopontin; as a target molecule for the treatment of inflammatory diseases. Curr Drug Targets 11:494–505.

Murakami I, Morimoto A, Oka T, Kuwamoto S, Kato M, Horie Y, Hayashi K, Gogusev J, Jaubert F, Imashuku S, Al-Kadar LA, Takata K, Yoshino T. 2013. IL-17A receptor expression differs between subclasses of Langerhans cell histiocytosis, which might settle the IL-17A controversy. Virchows Arch 462:219–228.

Porter AG, Janicke RU. 1999. Emerging roles of caspase-3 in apoptosis. Cell Death Differ 6:99–104.

Prasse A, Stahl M, Schulz G, Kayser G, Wang L, Ask K, Yalcintepe J, Kirschbaum A, Bargagli E, Zissel G, Kolb M, Müller-Quernheim J, Weiss JM, Renkl AC. 2009. Essential role of osteopontin in smoking-related interstitial lung diseases. Am J Pathol 174:1683–1691.

Redlich K, Hayer S, Ricci R, David JP, Tohidast-Akrad M, Kollias G, Steiner G, Smolen JS, Wagner EF, Schett G. 2002. Osteoclasts are essential for TNF-alpha-mediated joint destruction. J Clin Invest 110:1419–1427.

Rivollier A, Mazzorana M, Tebib J, Piperno M, Aitsiselmi T, Rabourdin-Combe C, Jurdic P, Servet-Delprat C. 2004. Immature dendritic cell transdifferentiation into osteoclasts: A novel pathway sustained by the rheumatoid arthritis microenvironment. Blood 104:4029–4037.

Smith LL, Cheung HK, Ling LE, Chen J, Sheppard D, Pytela R, Giachelli CM. 1996. Osteopontin N-terminal domain contains a cryptic adhesive sequence recognized by alpha9beta1 integrin. J Biol Chem 271:28485–28491.

Standal T, Borset M, Sundan A. 2004. Role of osteopontin in adhesion, migration, cell survival and bone remodeling. Exp Oncol 26:179–184.

Storgard CM, Stupack DG, Jonczyk A, Goodman SL, Fox RI, Cheresh DA. 1999. Decreased angiogenesis and arthritic disease in rabbits treated with an alphavbeta3 antagonist. J Clin Invest 103:47–54.

Teitelbaum SL. 2000. Bone resorption by osteoclasts. Science 289:1504–1508.

Tuck AB, Chambers AF, Allan AL. 2007. Osteopontin overexpression in breast cancer: Knowledge gained and possible implications for clinical management. J Cell Biochem 102:859–868.

Uede T. 2011. Osteopontin, intrinsic tissue regulator of intractable inflammatory diseases. Pathol Int 61:265–280.

Umekawa T, Tsuji H, Uemura H, Khan SR. 2009. Superoxide from NADPH oxidase as second messenger for the expression of osteopontin and monocyte chemoattractant protein-1 in renal epithelial cells exposed to calcium oxalate crystals. BJU Int 104:115–120.

Yamaguchi Y, Shao Z, Sharif S, Du XY, Myles T, Merchant M, Harsh G, Glantz M, Recht L, Morser J, Leung LL. 2013. Thrombin-cleaved fragments of osteopontin are overexpressed in malignant glial tumors and provide a molecular niche with survival advantage. J Biol Chem 1:3097–3111.

Yamamoto N, Nakashima T, Torikai M, Naruse T, Morimoto J, Kon S, Sakai F, Uede T. 2007. Successful treatment of collagen-induced arthritis in non-human primates by chimeric anti-osteopontin antibody. Int Immunopharmacol 7:1460–1470.

Yokosaki Y, Matsuura N, Sasaki T, Murakami I, Schneider H, Higashiyama S, Saitoh Y, Yamakido M, Taooka Y, Sheppard D. 1999. The integrin alpha(9)beta(1) binds to a novel recognition sequence (SVVYGLR) in the thrombin-cleaved amino-terminal fragment of osteopontin. J Biol Chem 274:36328–36334.

Yumoto K, Ishijima M, Rittling SR, Tsuji K, Tsuchiya Y, Kon S, Nifuji A, Uede T, Denhardt DT, Noda M. 2002. Osteopontin deficiency protects joints against destruction in anti-type II collagen antibody-induced arthritis in mice. Proc Natl Acad Sci USA 99:4556–4561.

SUPPORTING INFORMATION

Additional supporting information may be found in the online version of this article at the publisher's web-site.